COMPUTATIONAL SIMULATION OF NATURAL CONVECTION OF A MOLTEN CORE IN LOWER HEAD OF A PWR PRESSURE VESSEL

Camila Braga Vieira, camila@lasme.coppe.ufrj.br
Gabriel Alves Romero, gabrielromero@lasme.coppe.ufrj.br
Jian Su, sujian@lasme.coppe.ufrj.br
Universidade Federal do Rio de Janeiro, COPPE, Nuclear Engineering Program

Abstract *Computational simulation of natural convection in a molten core during a hypothetical severe accident in the lower head of a typical PWR pressure vessel was performed for two-dimensional semi-circular geometry with isothermal walls. Transient turbulent natural convection heat transfer of a fluid with uniformly distributed volumetric heat generation rate was simulated by using a commercial computational fluid dynamics (CFD) software ANSYS CFX 12.0. The Boussinesq model was used for the buoyancy effect generated by the internal heat source in the flow field. The two-equation k-ω based SST (Shear Stress Transport) turbulence model was used to mould the turbulent stresses in the Reynolds-Average Navier-Stokes equations (RANS). Two Prandtl numbers,* 6.13 *and* 7.0*, were considered. Five Rayleigh numbers were simulated for each Prandtl number used (*10^9*,* 10^{10}*,* 10^{11}*,* 10^{12}*, and* 10^{13}*). The average Nusselt numbers on the bottom surface of the semicircular cavity were in excellent agreement with Mayinger et al. (1976) correlation and only at* $Ra = 10^9$ *the average Nusselt number on the top flat surface was in agreement with Mayinger et al. (1976) and Kulacki and Emara (1975) correlations.*

Keywords: *heat transfer, turbulence models, SST, severe accident, natural convection*

1. INTRODUCTION

Natural convection has been studied in many different areas and its achievements have increased in nuclear engineering under the motivation of preventing a hypothetical severe accident in a nuclear power plant. In-vessel retention by flooding the reactor cavity and thus submerging the reactor vessel, has been studied intensively as a severe accident management concept (Theofanous et al., 1997). By externally cooling the lower head of the reactor pressure vessel, it targets to maintain the lower head integrity under the thermo-mechnical loads during the downward relocation of a molten core. The evaluation of the thermal load on the vessel lower head during the severe accident requires understanding and calculation of natural convection heat transfer of a heat generating fluid in hemispherical cavities.

The physical phenomenon of natural convection of a heat-generating fluid in a cavity is governed by two dimensionless parameters, the Rayleigh number Ra and Prandtl number Pr,

$$Ra = \frac{q_v g \beta H^5}{\alpha \nu k} \quad \text{and} \quad Pr = \frac{\nu}{\alpha} \tag{1}$$

where q_v is the internal heat generation rate, β the thermal expansion coefficient, α the thermal diffusivity, ν the kinematic viscosity, k the thermal conductivity, H the height of the cavity or the radius of a semicircular cavity.

Experimental and numerical studies on natural convection heat transfer of a heat generating fluid in three-dimensional hemispherical or two-dimension semicircular cavities have been carried out in last two decades. Kulacki and Emara (1975) studied natural convecction in a horizontal fluid layer boundary from above by a heat-conducting plate held at constant temperature and from below by an insulated plate. For Prandtl numbers varing from 2.75 to 6.85 and Rayleigh numbers up to 2×10^{12}, the experimental data of Kulacki and Emara (1975) were correlated by the following expression:

$$Nu_{top} = 0.403 Ra^{0.226} \tag{2}$$

Mayinger et al. (1976) obtained numerically and experimentally average Nusselt numbers on the bottom and top surfaces of a two-dimensional semi-circular slice cavity, with all cavity wall being cooled. The Prandtl number of the working fluid was 7.0. The Rayleigh number ranged from 10^7 to 5×10^{10}. The following correlations were obtained by fitting the experimental data, for the top and bottom surfaces respectively:

$$Nu_{top} = 0.36 Ra^{0.23} \tag{3a}$$

$$Nu_{bottom} = 0.54 Ra^{0.18} \tag{3b}$$

Asfia et al. (1996) conducted experiments to examine natural convection heat transfer in internally heated and partially filled spherical pools with external cooling. In the experiments, Freon-113 was contained in a Pyrex bell jar, which was externally cooled with subcooled water. Rayleigh numbers based on pool height ranged from 2×10^{10} to 1.1×10^{14}. Correlations for the local heat transfer coefficient dependence on pool angle and for the dependence of average Nusselt

number on Rayleigh number and pool depth were developed. It was found that dissimilar boundary conditions in the pool surface (free surface, insulated surface or cooled rigid surface) provoke only a slight difference in the average heat transfer coefficients. Their experimental data was in agreement with the correlation developed by Kulacki and Emara (1975).

Lee and Suh (2003) reported results from the Mini-SIGMA (Simulation of Internal Gravity-driven Melt Accumulation) tests with Rayleigh numbers up to 10^{10}. The test section was two-dimensional slice with 250 mm diameter, 125 mm height and 50 mm thickness. They concluded that the heat flux profile along the lower wall and average upward heat transfer with the Ra ranged from 10^7 to 10^{10} were in agreement with the data obtained from other numerical and experimental studies reported in the literature.

Many numerical simulations were also used to describe the behavior of natural convection in semicircular cavities. Dinh and Nourgaliev (1997) investigated numerically the natural convection heat transfer in a volumetrically heated liquid pool under high Rayleigh number (up to 10^{15}) with a low Reynolds k-ϵ model. The buoyancy-induced anisotropy of turbulence was modelled by means of the local Richardson number (Dinh and Nourgaliev, 1997). Phenomenological corrections were proposed for the turbulent Prandtl number and the near-wall viscosity, accounting for the effects of density and/or temperature stratification on turbulence. Loktionov et al. (1999) numerically investigated the reactor pressure behaviour under severe accident conditions taking into account the combined processes of vessel creep and the molten pool natural convection. Two-dimensional transient Navier-Stokes equations with a low Reynolds number turbulence model were solved for the prediction of natural convection in the molten pool.

This paper presents two-dimensional numerical simulations of turbulent natural convection in a fluid with internal heat generation uniformly distributed in a semicircular cavity with all isothermal walls. The simulations were executed at Rayleigh numbers in the range of 10^9 to 10^{13} and two Prandtl numbers were used in the analysis, 6.13 and 7.0. The turbulent flow was simulated with the shear stress tensor (SST) model, which is based in the Reynolds Average Navier-Stokes (RANS) equations. Based on numerical simulations, the distributions of Nusselt number on the bottom and top surfaces of the cavity were obtained and compared with empirical correlations presented in literature.

2. GOVERNING EQUATIONS

Turbulent natural convection was considered internal heat generation in a two-dimensional cavity. The Boussinesq model was used for the buoyancy due to small gradient pressure. In all other terms, except the buoyancy one, the density was considered constant as well as the specific heat, thermal conductivity and viscosity. The problem is illustrated by figure 1 and was governed by the following equations.

$$\nabla \cdot \mathbf{U} = 0 \tag{4}$$

where ρ is the density, $\mathbf{U}$ is the velocity vector and t is the time. The Reynolds averaged Navier-Stokes (RANS) equations are given by:

$$\rho\frac{\partial \mathbf{U}}{\partial t} + \rho\nabla\cdot(\mathbf{U}\otimes\mathbf{U}) = -\nabla p' + \nabla\cdot\left(\mu_{eff}(\nabla\mathbf{U}+\mathbf{U})^T\right) + \mathbf{B} \tag{5}$$

where $\mathbf{B}$ is the body force vector, given by the Boussinesq model, μ_{eff} is the effective viscosity and p' is the turbulent modified pressure with hydrostatic pressure at reference density reduced.

The turbulent modified pressure was defined by:

$$p' = p + \frac{2}{3}\rho k + \rho_{ref}\mathbf{g}(\mathbf{r}-\mathbf{r}_{ref}) \tag{6}$$

where p is pressure, k is the turbulence kinetic energy.

The effective viscosity is given by:

$$\mu_{eff} = \mu + \mu_t \tag{7}$$

where μ_t is the turbulent eddy viscosity and μ is the molecular viscosity of the fluid.

The SST turbulence model (*Shear Stress Transport*), defined by Menter (2003) and Menter et al. (2003), was used for turbulence modeling, which combines the advantages of the $k-\epsilon$ far from the wall and the $k-\omega$ near the wall. The transformed equations for the $k-\epsilon$ and the $k-\omega$ for SST turbulence model are:

$$\rho\frac{\partial k}{\partial t} + \rho\nabla\cdot(\mathbf{U}k) = \nabla\cdot[(\mu+\frac{\mu_t}{\sigma_{k2}})\nabla k] + P_k + P_{kb} - \beta'\rho k\omega \tag{8}$$

$$\rho\frac{\partial \omega}{\partial t} + \rho\nabla\cdot(\mathbf{U}\omega) = \nabla\cdot[(\mu+\frac{\mu_t}{\sigma_{\omega 3}})\nabla\omega] + (1-F_1)2\rho\frac{1}{\sigma_{\omega 2}\omega}\nabla k\nabla\omega + \alpha_3\frac{\omega}{k}P_k + P_{\omega b} - \beta_3\rho\omega^2 \tag{9}$$

where ω is the turbulence frequency and $\nu_t = \mu_t/\rho$. P_k is the shear production of turbulence and its limits are defined by:

$$P_k = \mu_t \nabla \mathbf{U} \left(\nabla \mathbf{U} + \nabla \mathbf{U}^T \right) \quad \rightarrow \quad \widetilde{P}_k = \min(P_k, 10\beta^* \rho k \omega) \tag{10}$$

For the Boussinesq model, the Buoyancy production term in the equation for turbulent kinetic energy P_{kb} was modeled by

$$P_{kb} = \frac{\mu_t}{\rho \sigma_\rho} \rho \beta \mathbf{g} \cdot \nabla T \tag{11}$$

The buoyancy production term in the ω equation was given by

$$P_{\omega b} = \frac{\omega}{k} \left((\alpha + 1) C_3 \max\left(P_{kb}, 0\right) - P_{kb} \right) \tag{12}$$

All the model constants were obtained through the combination of the corresponding constants of the $k - \epsilon$ and $k - \omega$ model using a blending function F_1 by $\alpha = \alpha_1 F_1 + \alpha_2 (1 - F_1)$, where α_1 e α_2 are constants of the models $k - \omega$ and $k - \epsilon$ respectively.

The constants for this model are: $\beta^* = 0,09$, $\alpha_1 = 5/9$, $\beta_1 = 3/40$, $\sigma_{kl} = 0,85$, $\sigma_{\omega l} = 0,5$, $\alpha_2 = 0,44$, $\beta_2 = 0,0828$, $\sigma_{k2} = 1$ e $\sigma_{\omega 2} = 0,856$.

The first blending function F_1 is defined by:

$$F_1 = \tanh\left\{ \left\{ \min\left[\max\left(\frac{\sqrt{k}}{\beta^* \omega y}, \frac{500\nu}{y^2 \omega} \right), \frac{4\rho\sigma_{\omega 2} k}{CD_{k\omega} y^2} \right] \right\}^4 \right\} \tag{13}$$

where $CD_{k\omega}$ is

$$CD_{k\omega} = \max\left(2\rho\sigma_{\omega 2} \frac{1}{\omega} \nabla k \bullet \nabla \omega, 10^{-10} \right) \tag{14}$$

and y is the distance to the nearest wall.

F_1 is equal to zero away from the surface ($k - \epsilon$ model), and switches to one inside the boundary layer ($k - \omega$ model). The turbulent eddy viscosity is defined as:

$$\nu_t = \frac{a_1 k}{\max(\quad a_1 \omega, S F_2)} \tag{15}$$

where $a_1 = 0,31$, S is the invariant measure of strain rate given by $\sqrt{2\mathbf{D} : \mathbf{D}}$ and F_2 is a second blending function defined by:

$$F_2 = \tanh\left[\left[\max\left(\frac{2\sqrt{k}}{\beta^* \omega y}, \frac{500\nu}{y^2 \omega} \right) \right]^2 \right] \tag{16}$$

This model requires knowledge of the distance between nodes and nearest wall. Hence, a better interaction between the $k - \omega$ and $k - \epsilon$ is obtained . The wall scale equation is solved to get these wall distances:

$$\nabla^2 \phi = -1 \tag{17}$$

where ϕ is the value of the wall scale. The wall distance can be calculated from the wall through:

$$WD = \sqrt{|\nabla \phi|^2 + 2\phi} - |\nabla \phi| \tag{18}$$

The mathematical model was numerically solved by using the commercial CFD package *ANSYS CFX-12.0*. This program uses numerical method of finite volume as solution (Element Based Finite Volume Method - EBFVM), which allows the resolution of problems even in unstructured grids. Therefore, it is possible to obtain a numerical solution of discretized momentum and mass balance equations.

3. PHYSICAL PROBLEM AND SIMULATION PROCEDURE

Numerical simulations were executed to analyze natural convection heat transfer of a heat-generating fluid in a two-dimensional semi-circular slice covered with a rigid conducing flat wall, as shown in Fig. 1. The bottom semi-circular surface and the top flat surface were kept at a same constant temperature T_0 ($293\ K$), which is also used as the reference temperature of the buoyancy term. Two Prandtl numbers were considered, 6.13 and 7.0 and five Rayleigh numbers were simulated for each Prandtl number: 10^9, 10^{10}, 10^{11}, 10^{12}, and 10^{13}.

The average Nusselt number studied is defined as follows,

$$\bar{N}u = \frac{\bar{q}_w H}{k(T_{av} - T_0)} \tag{19}$$

in which $\bar{q}_w$ is the average heat flux on the bottom or top surface and T_{av} is the average temperature in the cavity.

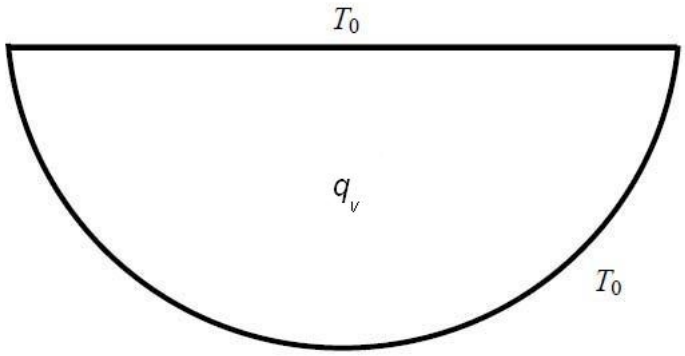

Figure 1. Scheme of the problem analysed

4. RESULTS AND DISCUSSION

A grid independence analysis was accomplished before the obtainment of results. The heat transfer in the bottom of the cavity was analyzed for four grids. Table 1 shows the statistics of the meshes used in the mesh sensivity procedure executed for $Pr = 7$ and $Ra = 10^{16}$.

Table 1. Mesh statistics used in the grid independece analyzis.

	Grid 1	Grid 2	Grid 3	Grid 4
Number of nodes	11816	50328	100460	208928
Number of elements	5828	24989	49982	104115

The differences between the computed Nusselt numbers for the grids are shown Table 2. The grid used in the numerical simulations was the grid-3, since it is a fine mesh and does not require so much computational effort like grid-4.

Table 2. Mesh sensivity: differences between the avarege of the Nusselt number around the bottom of the semicircular cavity to $Pr = 7$ and $Ra = 10^{16}$

	Difference (%)
Grid 1 to 2	2.98
Grid 2 to 3	2.11
Grid 3 to 4	1.21

The local heat transfer around the bottom is shown in Fig. 2 in which the local distribution of wall-average Nusselt numbers are presented.

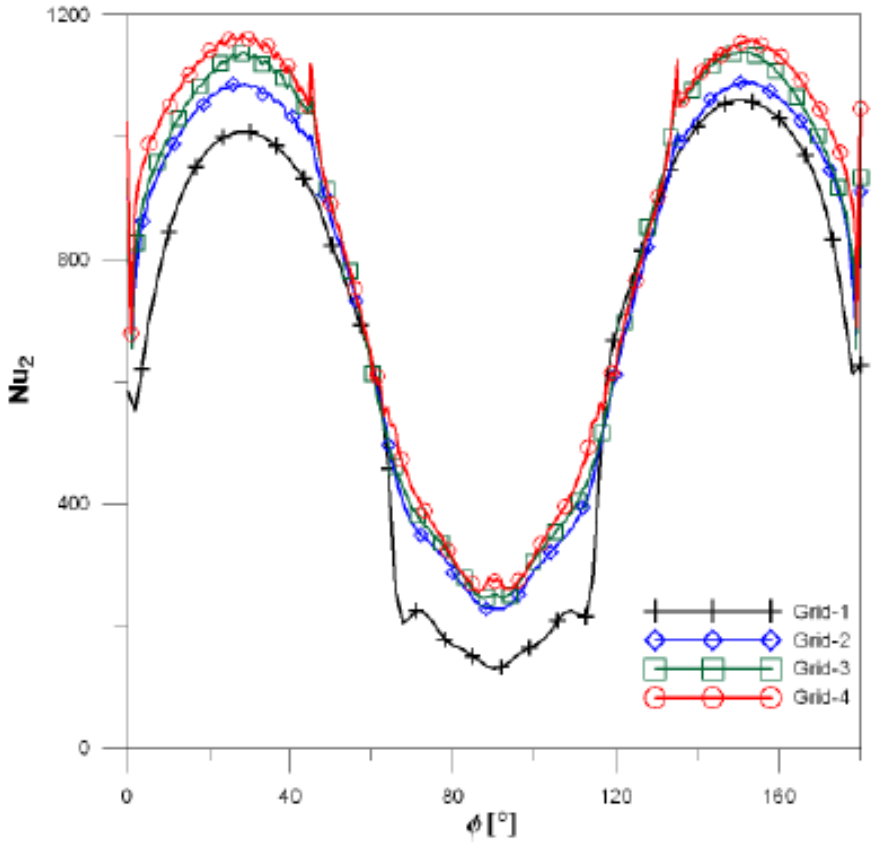

Figure 2. Local distribution of averaged Nusselt number around the bottom the semi-circular cavity for $Pr = 7.0$ and $Ra = 10^{16}$

As can be seen in Figure 3, the Nusselt numbers on the bottom surface obtained by the present simulation are in excellent agreement with the empirical correlation proposed by Mayinger et al. (1976) that fitted their experimental data with $Pr = 7.0$ and Rayleigh number ranging from 10^7 to 5×10^{10}. The Nusselt numbers for $Pr = 6.13$ slightly deviated from the experimental correlation, showing a weak Prandtl number dependency at lower Rayleigh numbers ($Ra = 10^9$ and $Ra = 10^{10}$) on the investigated range. After $Ra = 10^{11}$ there was splendid agreement between the numerical results and the correlation, for both Prandtl numbers. A slight deviation appeared at $Ra = 10^{13}$, which indicates that the Mayinger et al. (1976) correlation, developed for lower Rayleigh numbers, may not be applicable for Rayleigh number higher than 10^{13}. On the other hand, the agreement between the Nusselt numbers on top flat surface obtained by the present numerical simulation and two empirical correlations was not as good as the agreement for bottom surface average Nusselt numbers. There was an excellent agreement between the calculated average top surface Nusselt number and the Mayinger et al. (1976) and the Kulacki and Nagle (1975) correlations only for $Ra = 10^9$.

For higher Rayleigh numbers, the calculated Nusselt numbers were systematically lower than the values given by the empirical correlations. Comparing the results, the numerical results can be considered acceptable based on the agreement on the bottom surface and the on top surface at $Ra = 10^{10}$. If the Mayinger et al. (1976) correlation for the bottom surface is accurate and reliable and there is a good agreement between the numerical results and the correlation, the numerically calculated average top Nusselt number should also be accurate and reliable, as a consequence of energy conservation. The numerical simulation indicated a lower increasing rate of the Nusselt number as a function of the Rayleigh number, which should be reasonable from a physical point of view.

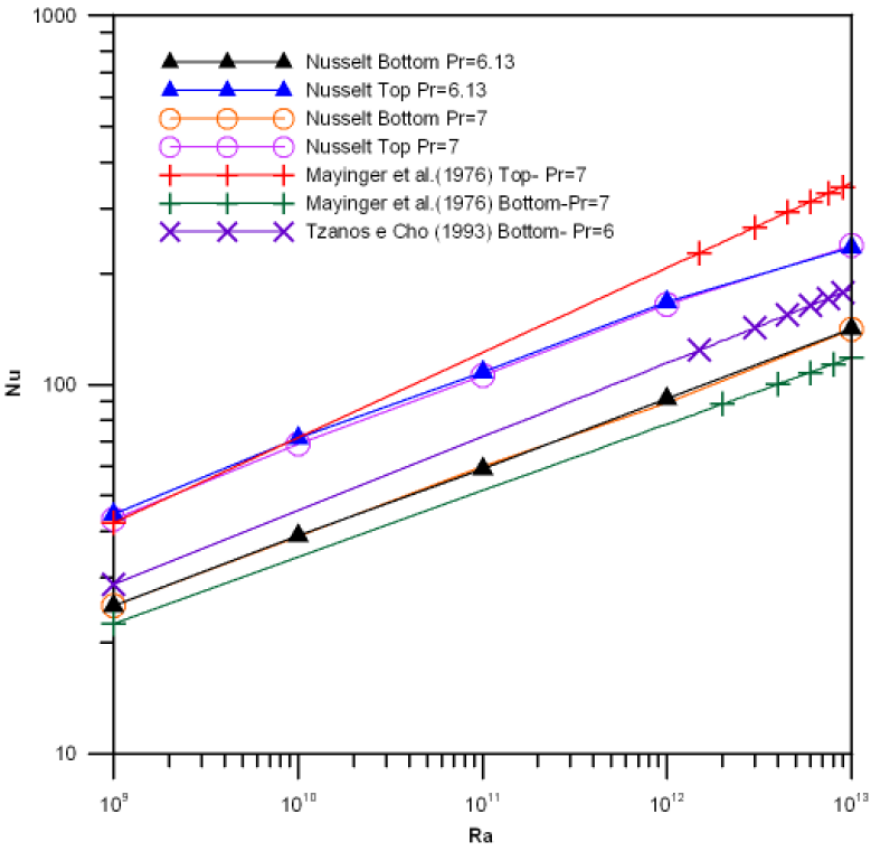

Figure 3. Nusselt numbers as a function of Rayleigh number for $Pr = 6.13$ and $Pr = 7.0$.

Instantaneous velocity and temperature fields obtained by the present numerical simulations are shown in Fig. 4 to 7 for $Pr = 7.0$ and $Ra = 10^9$, 10^{10}, 10^{11}, 10^{12}, and 10^{13}. A literature result of temperature field for $Pr = 7.0$ and $Ra = 10^{12}$ is shown in Figure 8 for comparison. It can be observed that there is a steady stratification at the bottom of the semicircular cavity for lower Rayleigh number, which becomes gradually smaller with increasing Rayleigh number. At lower Rayleigh number, the heat transfer mechanism near the bottom of the cavity is dominated by the α-phenomena, defined by Nourgaliev et al. (1997), where heat conduction is the dominant mechanism of heat transfer in the strongly stably stratified layers at the bottom surface. The ν-phenomena can be clearly seen in Fig. 6 and 7 where the descending fluids penetrate, at the peripheral regions, into the stably stratified layers. It can also be noticed that with increasing Rayleigh number, the temperature distribution in the cavity becomes more uniform (for $Ra = 10^9$, $\theta_{max}/\theta_{av} = 1.363$, while for $Ra = 10^{13}$, $\theta_{max}/\theta_{av} = 1.051$). The homogenization of the temperature in the cavity may be explained by the increasing turbulent mixing in the cavity, as can been seen from the velocity fields shown in Fig. 4, 5, 6, and 7.

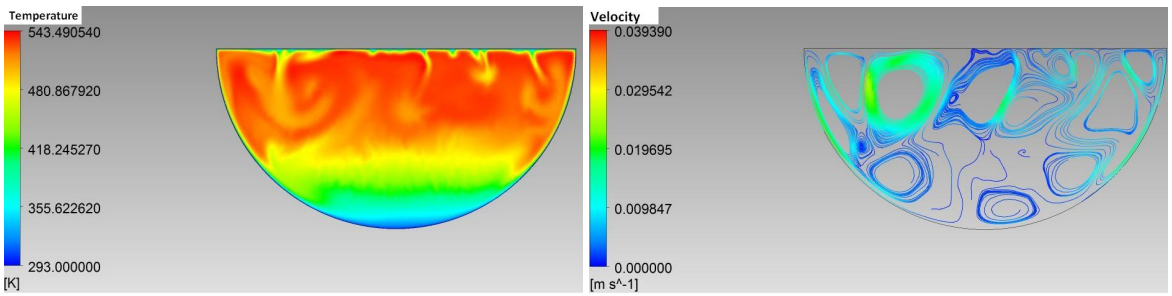

(a) (b)

Figure 4. Temperature field (a) and Velocity field (b) for $Pr = 7.0$ and $Ra = 10^{10}$

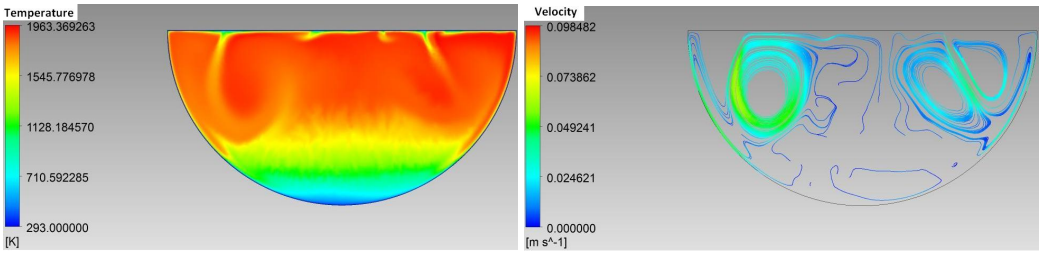

(a) (b)

Figure 5. Temperature field (a) and Velocity field (b) for $Pr = 7.0$ and $Ra = 10^{11}$

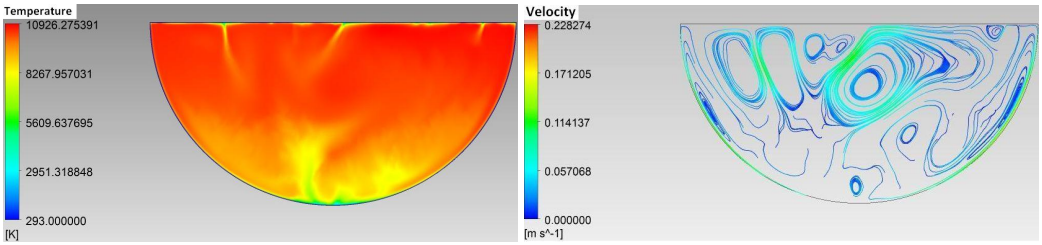

(a) (b)

Figure 6. Temperature field (a) and Velocity field (b) for $Pr = 7.0$ and $Ra = 10^{12}$

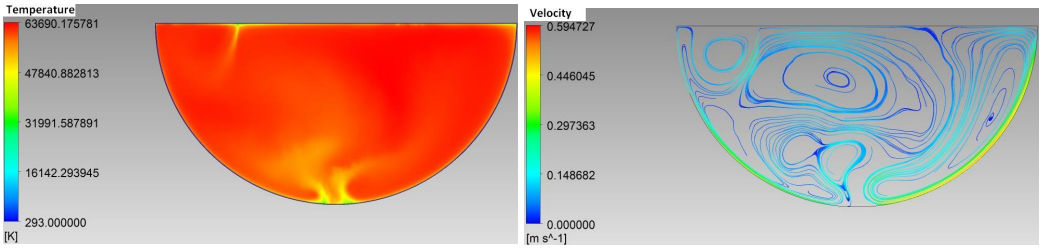

(a) (b)

Figure 7. Temperature field (a) and Velocity field (b) for $Pr = 7.0$ and $Ra = 10^{13}$

5. CONCLUSIONS

The average Nusselt numbers on the bottom surface calculated by the computational simulations were in excellent agreement with Mayinger et al. (1976) and Kulacki and Nagle (1975) correlations only at $Ra = 10^9$. For higher Rayleigh numbers, the calculated Nusselt numbers were systematically lower than the values given by the empirical correlations. Comparing the results, the numerical ones can be considered good based on the bottom surface and the agreement on top surface at $Ra = 10^{10}$. Numerical results of the velocity and temperature fields showed the α-phenomena and ν-phenomena, defined by Nourgaliev et al. (1997). The α-phenomena was predominant at lower Rayleigh number, in which heat conduction was the dominant mechanism of heat transfer in the strongly stably stratified layers at the bottom surface. The ν-phenomena could be clearly seen in Fig. 6 and 7 where the descending fluids penetrate, at the peripheral regions, into the stably stratified layers. For $Ra = 10^9$, $\theta_{max}/\theta_{av} = 1.363$, while for $Ra = 10^{13}$, $\theta_{max}/\theta_{av} = 1.051$, concluding that with increasing Rayleigh number, the temperature distribution in the cavity become more uniform.

6. ACKNOWLEDGEMENTS

The authors gratefully acknowledge financial support provided by CNPQ during the realization of this work.

7. REFERENCES

Asfia, F. J., Frantz, B., and Dhir, V. K. (1996). Experimental investigation of natural convection heat transfer in volumetrically heated spherical segments. *Journal of Heat Transfer-Transactions of the Asme*, 118(1):31–37.

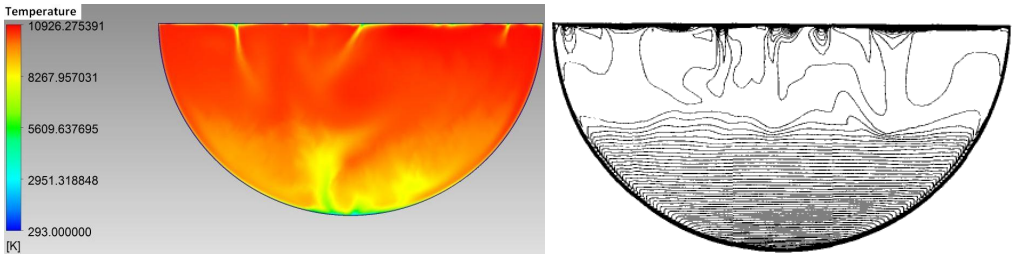

(a) (b)

Figure 8. Temperature field obtained by this work (a) and temperature field of literature(b) for $Pr = 7.0$ and $Ra = 10^{12}$.

Dinh, T. and Nourgaliev, R. (1997). Turbulence modelling for large volumetrically heated liquid pools. *Nuclear Engineering and Design*, 169:131–150.

Kulacki, F. A. and Emara, A. A. (1975). High rayleigh number convection in enclosed fluid layers with internal heat sources. Technical Report NUREG-75/065, U.S. Nuclear Regulatory Commission Report.

Kulacki, F. A. and Nagle, M. E. (1975). Natural-convection in a horizontal fluid layer with volumetric energy-sources. *Journal of Heat Transfer-Transactions of the Asme*, 97(2):204–211.

Lee, S. and Suh, K. (2003). Natural convection heat transfer in two-dimensional semi-circular slice pool. *Journal of NUCLEAR SCIENCE and TECHNOLOGY.*, 40(10):775–782.

Loktionov, V. D., Mukhtarov, E. S., Yaroshenko, N. I., and Orlov, V. E. (1999). Numerical investigation of the reactor pressure vessel behaviour under severe accident conditions taking into account the combined processes of the vessel creep and the molten pool natural convection. *NUCLEAR ENGINEERING AND DESIGN*, 191(1):31–52.

Menter, F. (2003). Turbulence modelling for turbomachinery. In *QNET-CFD Network Newsletter*, volume 2, pages 10–13.

Menter, F. R., Kuntz, M., and Langtry, R. (2003). Ten years of industrial experience with the sst turbulence model. in K. Hanjalic, Y. Nagano e M. Tummers (eds.), *Turbulence, Heat and Mass Transfer 4*, Begell House, Inc.

Nourgaliev, R., Dinh, T., and Sehgal, B. (1997). Effect of fluid prandlt number on heat transfer characteristics in internally heated liquid pools with rayleigh numbers up to 10^{12}. *Nuclear Engineering and Design*, 169:165–184.

Theofanous, T. G., Liu, C., Additon, S., Angelini, S., Kymalainen, O., and Salmassi, T. (1997). In-vessel coolability and retention of a core melt. *Nuclear Engineering and Design*, 169(1-3):1–48.

8. Responsibility notice

The authors are the only ones responsible for the printed material included in this paper.